

Performance evaluation of Mn and Fe doped $\text{SrCo}_{0.9}\text{Nb}_{0.1}\text{O}_{3-\delta}$ cathode for IT-SOFC application

Lokesh Bele¹, R K Lenka², P K Patro², L Muhmood¹, T Mahata² and P K Sinha²

¹ K J Somaiya College of Engineering, Vidyavihar, Mumbai, India

² Powder Metallurgy Division, Bhabha Atomic Research Centre, Mumbai, India

E-mail: lokeshbele12@gmail.com, lokesh.bele@somaiya.edu

Abstract:

Cathode materials of Mn and Fe doped $\text{SrCo}_{0.9}\text{Nb}_{0.1}\text{O}_{3-\delta}$, are synthesized by solid state route for intermediate temperature fuel cell applications. Phase pure material is obtained after calcining the precursors at 1100 °C. Phase compatibility is observed between this novel cathode material with gadolinia doped ceria (GDC) electrolyte material as reflected in the diffraction pattern. The state of art YSZ electrolyte is not compatible with this cathode material. Average thermal expansion coefficient of the material varies between 17 to 22 X 10⁻⁶ K⁻¹ on doping, from room temperature to 800 °C. Increase in thermal expansion coefficient is observed with Mn and Fe doping associated with the loss of oxygen from the crystal. The electrical conductivity of the cathode material decreases with Fe and Mn doping. Mn doped samples show lowest conductivity. From the symmetric cell measurement lower area specific resistance (0.16 Ω-cm²) is obtained for un-doped samples, at 850 °C. From the initial results it can be inferred that Mn/Fe doping improves neither the thermal expansion co-efficient nor the electrochemical activity.

1. Introduction

In the quest for reliable and clean energy source, fuel cell has offered a promising technology towards direct conversion of chemical energy of fuel to electrical energy without any intermediate steps [1-2]. Solid oxide fuel cell (SOFC) has shown great advantages with respect to its high efficiency and fuel flexibility compared to other types of fuel cell. In a fuel cell, high temperature operation leads to better kinetics and performance. However, chemical compatibility of cell components, inter-diffusion of chemical species, chemical stability of construction materials and usefulness of sealing are the issues associated with the high temperature operation [3,4]. Lowering the operating temperature suppresses the degradation of cell components and thereby increases the durability of the cell and widens the choice of materials in stack design. However, operation of SOFC at lower temperature implies lower electrode kinetics, resulting in large interfacial polarization resistance especially the oxygen reduction reaction (ORR) at the cathode. Hence, over the last decade thrust has been given to develop SOFC that can be operated in the intermediate temperature range without sacrificing the performance. This challenge has been mitigated by various research groups worldwide through the development of new materials. Many mixed ionic and electronic (MIEC) conductors shown good performance as the dual ion and electron transfer capabilities extends the three-phase boundary away from the electrode-electrolyte interface. Few cathode compositions like $\text{Ba}_{0.5}\text{Sr}_{0.5}\text{Co}_{0.8}\text{Fe}_{0.2}\text{O}_{3-\delta}$ (BSCF), $\text{Sm}_{0.5}\text{Sr}_{0.5}\text{CoO}_{3-\delta}$,



$\text{SrCo}_{0.9}\text{Nb}_{0.1}\text{O}_{3-\delta}$ and $\text{SrSc}_{0.2}\text{Co}_{0.8}\text{O}_{3-\delta}$ have proven to be a candidate cathode material for IT-SOFC applications [5-8]. There are still some pros and cons of these types of cathode materials with respect to their stability in the operating condition and compatibility with other cell components. The higher catalytic activity of $\text{SrCoO}_{3-\delta}$ has paid much attention for the use as a SOFC cathode and oxygen permeation membrane [9]. Oxygen vacancies are developed at the A-site of the perovskite and a lower binding energy of the small size cobalt with oxygen facilitates fast oxygen diffusion in the bulk of the lattice. This also enhances the oxygen exchange kinetics on the surface of the cathode. However, the stability of the material and compatibility with the commonly used electrolyte materials (YSZ, GDC, LSGM, etc) is a matter of concern. Stability of the structure can be improved by suitably doping at A-site and B-site of the perovskite with suitable dopants. Substitution at B-site has been adopted by Nagai et.al and Nb is the most effective dopant among the others (Cr, Fe, Al, Ga, Ti, Zr, Sn, V and Nb) for phase stabilization in a $\text{SrCoO}_{3-\delta}$ system [10]. High oxygen permeability has been observed in case of Nb-doped $\text{SrCoO}_{3-\delta}$ perovskite oxides and has been used in the oxygen separation membranes. This Nb doping not only stabilizes the cubic perovskite crystal structure of $\text{SrCoO}_{3-\delta}$ oxide, but also the electronic and ionic conductivity at intermediate temperature region [11]. $\text{SrCoO}_{3-\delta}$ cathode was co-doped with Nb and Fe for better stability in CO_2 environment [12]. Effect of Mn substitution on the performance of $\text{SrCoO}_{3-\delta}$ has not been studied so far. In this present investigation Fe and Mn is co-doped with Nb to evaluate the performance as SOFC cathode.

2. Materials and methods

Three compositions, $\text{SrCo}_{0.9}\text{Nb}_{0.1}\text{O}_{3-\delta}$ (SNC), $\text{SrCo}_{0.8}\text{Mn}_{0.1}\text{Nb}_{0.1}\text{O}_{3-\delta}$ (SNMC) and $\text{SrCo}_{0.8}\text{Fe}_{0.1}\text{Nb}_{0.1}\text{O}_{3-\delta}$ (SNFC) were synthesized by solid-state reaction route using SrCO_3 , MnO_2 , Nb_2O_5 , Fe_2O_3 , and Co_3O_4 (Sigma-Aldrich) as the precursor materials. Required amount of the raw materials were mixed properly in a mortar and pestle followed by calcination at 1100 °C in air for 15 hours to form the perovskite oxide. The desired phase was confirmed from the powder X-ray diffraction (XRD) analysis on an INEL instrument using the $\text{Cu-K}\alpha$ radiation at 40 kV and 30 mA. This diffraction measurement was taken with a monochromatic radiation at a slit width of 0.15 mm with continuous counting from 10-120 degree. Compatibility of these cathodes with YSZ and GDC electrolyte was examined by X-ray diffraction study. Electrolyte powders with cathode material in 1:1 weight ratio were compacted in pellet form and heated at 1100 °C for 2 hours and diffraction pattern for the same was taken.

Thermal analysis of the sample was carried out using Setsys Evolution (SETARAM) thermal analyzer, from room temperature to 900 °C at a heating and cooling rate of 10 °C/min in flowing air. Thermal expansion measurement of cathodes was carried out in the form of cylindrical pellet prepared by uniaxial die pressing followed by sintering to near theoretical density. The cathode material was sintered at 1150 °C in air to get a dense sintered pellet. Expansion measurements were carried out using a dilatometer (Model: Setsys Evolution 2000) from room temperature to 800 °C in flowing air environment.

For conductivity measurement, rectangular bar shaped samples were prepared using a rectangular die followed by sintering at 1150 °C. Platinum grooves are made at 1 cm apart to fix the voltage probe in a 4-probe electrical conductivity measurement. The sintered density of the specimen is over 95% of the theoretical density as reflected from water displacement method. Platinum paste was applied on the opposite faces of the bar pellet to form the current electrode. The electrical conductivities were measured by a 4-probe DC technique using a probostat test unit from room temperature to 800 °C.

The electrochemical performance of novel SNC based cathode was evaluated in the form of symmetric cell configuration using yttria stabilized zirconia (YSZ) as an electrolyte. For the preparation of symmetric cells with the SNC||YSZ||SNC configuration, sintered YSZ pellets of 15.0 mm in diameter and 1.5 mm in thickness, were prepared through uniaxial die pressing followed by sintering at 1350 °C for 5 hours. Slurry of the SNC cathode material was prepared in terpinol medium (Terpinol:SNC = 1:1

by weight) and was coated over the dense YSZ pellet using a painting brush. This cathode layer was sintered at 950 °C for 1 hour. The thickness of the cathode was controlled by the number of coatings. Silver paste was applied to the opposite faces of the symmetric cells as a current collector. Solartron impedance analyser was used to collect the electrochemical impedance spectra (EIS) of the symmetric cells from 500 to 850 °C in static air. The impedance measurements were carried out under open cell voltage conditions from frequency range 0.01 Hz to 1.0 MHz with a signal amplitude was 10 mV. The result of the symmetric cell measurement was analysed using Z-view software (Scribner associates) and fitting the result to appropriate equivalent circuit.

3. Results and discussion

3.1 Phase characterization and compatibility

X-ray diffraction pattern of the SNC, SNFC and SNMC prepared through solid state route and calcined at 1100 °C for 15 hours is shown in figure 1. All the peaks in the X-ray diffraction pattern could be indexed to the $\text{SrSc}_{0.175}\text{Nb}_{0.025}\text{Co}_{0.8}\text{O}_{3-\delta}$ type perovskite phase as reported in the literature [13]. No extra peak has been observed in the X-ray diffraction pattern showing phase purity of the material. Compatibility of the SNC cathode with GDC electrolyte and YSZ electrolyte is revealed in figure 2a and 2b, showing the X-ray diffraction pattern of 1:1 mixture of the cathode and electrolyte heated at 1100 °C for 2 hours. Peaks corresponding to the cathode and the electrolyte were clearly demarcated. Apart from the electrolyte and the cathode peaks, no extra peaks have been detected from the diffraction pattern showing compatibility of the GDC with SNC cathode material. However, few extra peaks have been detected and highlighted in the diffraction pattern of YSZ-SNC mixture after heat treatment. This shows that YSZ is not much compatible to SNC based cathode material compared to GDC electrolyte. Stability of GDC electrolyte with SNFC is also confirmed by Wang et.al in a recent report [14].

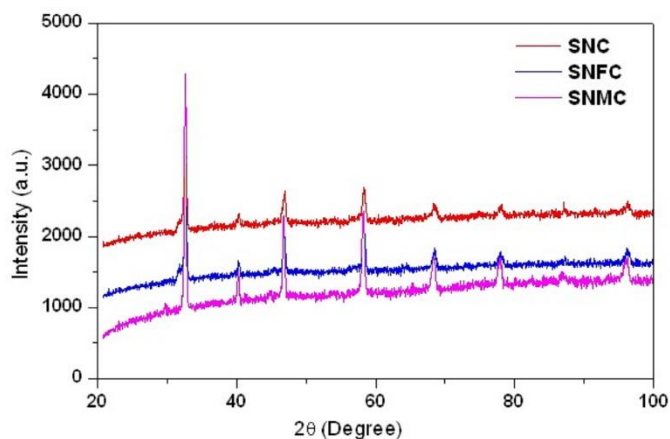


Figure 1. X-ray Diffraction pattern of SNC, SNFC and SNMC.

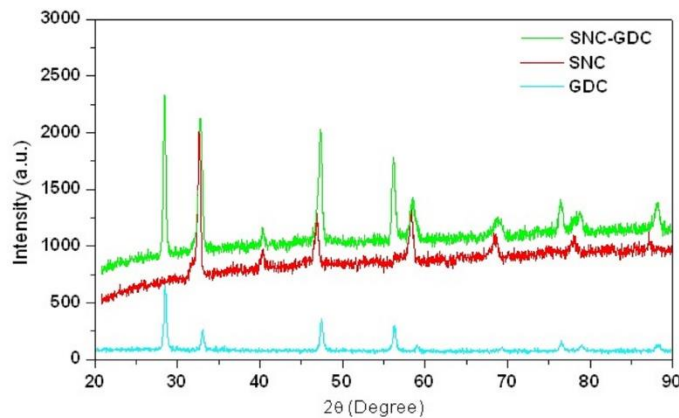


Figure 2a. X-ray Diffraction pattern SNC, GDC and their mixture after heat treatment.

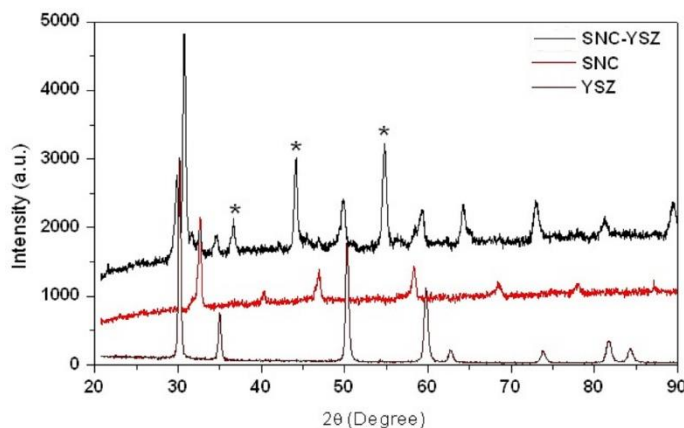


Figure 2b. X-ray Diffraction pattern SNC, YSZ and their mixture after heat treatment.

3.2 Thermal analysis and expansion

To observe the variation in oxygen non-stoichiometry in SNC based cathodes, figure 3 shows the thermogravimetric analysis (TGA) plot reflecting the changes in weight in percentage with temperature. The experiment was carried out from room temperature to 900 °C at a heating and cooling rate of 10 °C/min. The SNC based cathode materials experience a weight loss after 400 °C. This weight loss is associated with oxygen loss from the lattice. The total oxygen loss from room temperature to 900 °C is around 0.6%, equivalent to ~2.4% of total oxygen content. It is observed from the X-ray diffraction pattern that cathodes after TGA experiment retain the perovskite phase. Oxygen loss is more prominent in Fe doped SNC sample compared to Mn doped sample. Thermal expansion of the material from room temperature to 900 °C in static air environment is shown in figure 4. The average thermal expansion coefficient (TEC) of doped SNC from room temperature to 800 °C varies from 17 to 22 $\times 10^{-6} \text{ K}^{-1}$ as calculated from the expansion curve. The TEC is high compare to the GDC electrolyte material. However, composite electrode approach can be adopted to decrease the TEC of the cathode material. Increase in thermal expansion with Fe doping is indicated by Zhu et.al [15]. There is an appreciable change in the thermal expansion coefficient of these materials from room

temperature to high temperature. Increase in the thermal expansion coefficient is higher at higher temperature region compared to lower temperature region. The variation in thermal expansion coefficient is attributed to the loss of oxygen from the lattice, which leads to increase in the thermal expansion of the material. The change in slope of the thermal expansion curve corroborates the thermogravimetric data.

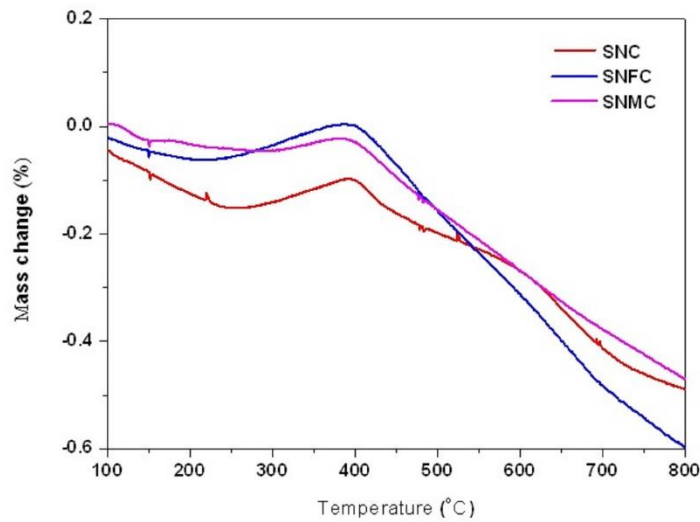


Figure 3. Thermogravimetric analysis (TGA) curve of SNC, SNFC and SNMC.

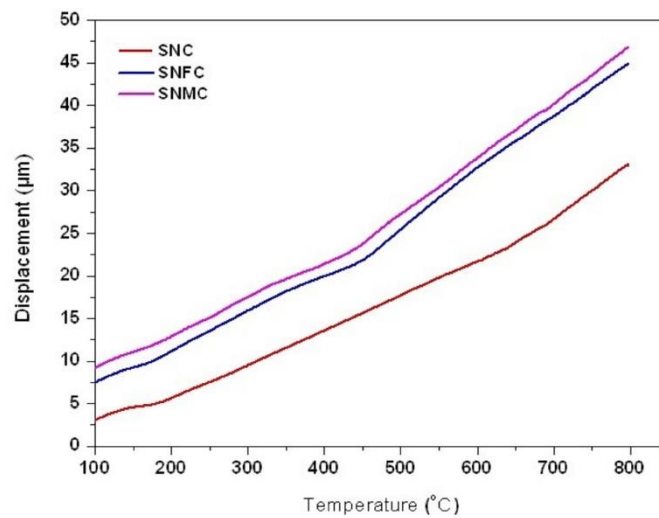


Figure 4. Thermal expansion of SNC, SNFC and SNMC with temperature.

Table 1. TEC values of cathode materials at 800 °C.

Composition	α ($10^{-6}/^{\circ}\text{C}$)	α ($10^{-6}/^{\circ}\text{C}$) (literature)	Reference
SNC	17.1	24.2	[11]
SNFC	21.7	26.4	[15]
SNMC	22.5	-	-

3.3 Electrical conductivity

DC- electrical conductivities of SNC, SNFC and SNMC are shown in figure 5. In all the samples, there is an increase in the conductivity value with temperature due to small polaron hopping conduction. The peak in the conductivity value lies between 350 to 400 °C. With further increase in temperature the conductivity value decreases. Similar trend is observed by Wang et.al [11]. A semiconducting to metallic type transition is observed after a temperature of 370 °C for SNC cathode material. Reduction in the valency state of Co^{4+} to Co^{3+} takes place at higher temperature along with loss of oxygen from the lattice as reflected from the thermal analysis data. In the low temperature region hole is the dominating charge carrier and responsible for the conduction mechanism. Beyond this temperature, oxygen vacancies are generated due to loss of oxygen from the lattice. Holes are annihilated due to the presence of oxygen vacancies and responsible for the decrease in the conductivity value [11]. It has been observed that conductivity decreases with Fe and Mn doping. This can be explained based on the decrease in the bond angle and increase in polaron binding energy [16]. At the same time, concentration of holes decreases with Fe and Mn doping due to the formation of oxygen vacancy. Conductivity maximum of SNC and SNFC reported in the literature are 460 and 304 S cm^{-1} respectively [11,15]. Sufficient electrical conductivity, more than 50 S cm^{-1} is obtained for all samples in the operating temperature region of the fuel cell.

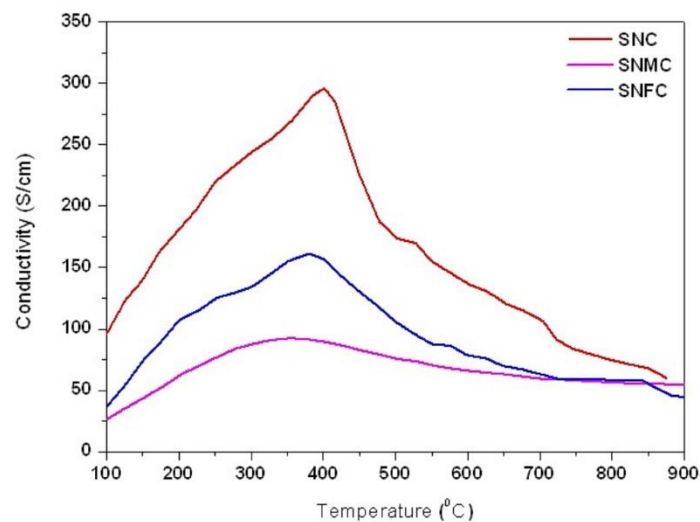


Figure 5. DC-conductivity as function of temperature for SNC, SNFC and SNMC.

3.4 Oxygen reduction reaction (ORR) from the symmetric cell measurement

The catalytic property of a cathode material for the oxygen reduction reaction at the cathode-electrolyte interface is expressed in terms of area specific polarization resistance (ASR) or R_p . The

polarization resistance is obtained from impedance measurement of a symmetric cell with the same electrode applied at both sides of the electrolyte. This polarization resistance is obtained from the difference in intercepts of the impedance curve to the real axis. This result is corrected for each surface and the area of the cathode surface used for measurement. Temperature dependant area specific polarization resistance (ASR) of SNC based cathodes is shown in figure 6a-c. ASR of SNC, SNFC and SNMC are 0.165, 0.5 and 1.6 $\Omega\text{-cm}^2$ at 850 °C, respectively. This shows that SNC cathode can perform well in the intermediate temperature region. Similar ASR has been reported in the literature for SNC and SNFC [11]. Figure 7 shows the microstructure of the cathode-electrolyte interface for SNC based symmetric cell. Microstructure for one composition is shown here for representation. Good adherence at the interface and enough porosity in the cathode is observed in the micrograph. This shows that SNC cathode can perform well in the intermediate temperature region.

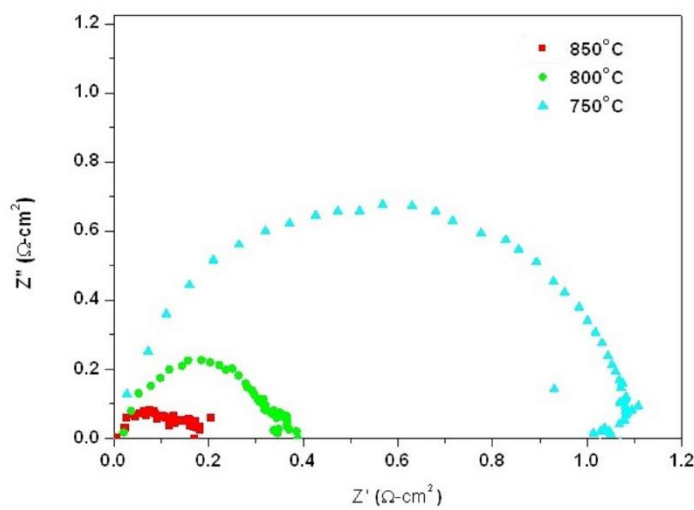


Figure 6a. Variation of ASR with temperature for SNC cathode.

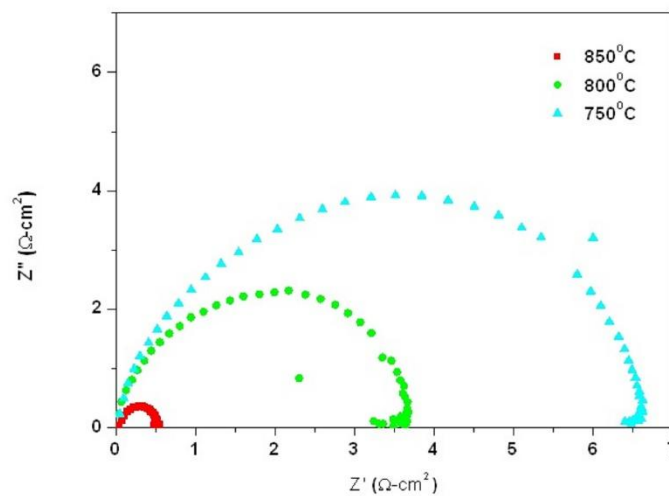


Figure 6b. Variation of ASR with temperature for SNFC cathode.

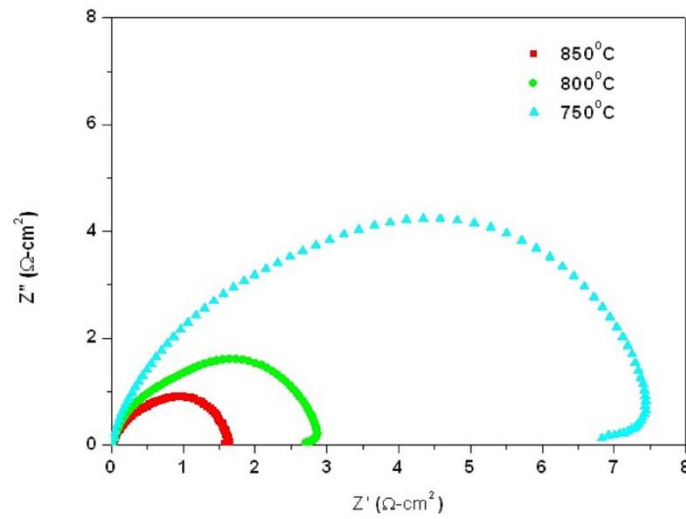


Figure 6c. Variation of ASR with temperature for SNMC cathode.

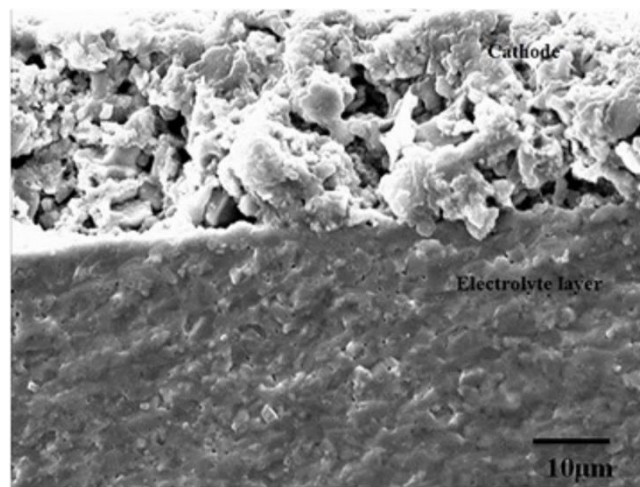


Figure 7. Microstructure of cathode-electrolyte interface in SNC based symmetric cell.

4. Conclusion

Phase pure SNC, SNFC and SNMC have been synthesized by solid state route by mixing the individual components and subsequently calcining the mixture at 1100 °C. There is a good compatibility between SNC and GDC electrolyte material. The thermal expansion coefficient of SNC cathode remains higher in comparison to GDC electrolyte and increases with Fe and Mn doping. The electrical conductivity increases with increase in temperature up to 400 °C and decreases with further increases in temperature. Conductivity above 50 S cm⁻¹ has been obtained in the operating temperature

region of fuel cell (500-800 °C). The area specific resistance of the interface between the new cathode and GDC electrolyte material is reasonably low and the value can be further brought down through optimization of process parameters. The results suggest that SNC forms a candidate material for application as SOFC cathode material.

References

- [1] Vielstich W, Gasteiger H A and Lamm A (Editors) *Hand book of fuel cells, Fundamentals, Technology and applications* John Wally & Sons Chichester, England, 2003, ISBN 0-471-49926-9
- [2] Debaer B, *PhD Thesis*, University of Twente, the Netherlands
- [3] Sun C, Hui R and Roller J 2010 *J. Solid State Electrochem.* **14** 1125–44
- [4] Hui R, Sun C, Yick S, Deces-Petit C, Zhang X, Maric R and Ghosh D 2010 *Electrochim. Acta* **55** 4772–75
- [5] Shao Z P and Haile S M 2004 *Nature* **431** 170
- [6] Hibino T, Hasimoto A, Inoue T, Tokuno J, Yoshida S and Sano M 2000 *Science* **288** 2031
- [7] Zhou W, Shao Z P, Ran R, Jin W Q and Xu N P 2008 *Chem. Commun.* 5791-93
- [8] Zhou W, Shao Z P, Ran R and Cai R 2008 *Electrochem. Commun.* **10**, 1647-51
- [9] Zhang K, Ran R, Ge L, Shao Z, Jin W and Xu N 2008 *J. Membrane Science* **323** 436–43
- [10] Nagai T, Ito W and Sakon T 2007 *Solid State Ionics* **177** 3433-44
- [11] Wang F, Zhou Q, He T, Li G and Ding H 2010 *J. Power Sources* **195** 3772-78
- [12] Lu H, Kim J P, Son S H and Park J H 2011 *Mater.Lett.* **65** 2558-60
- [13] *Angew. Chem.* 2013 **125** 14286 –290
- [14] Wang S, Jin F, Li L, Li R, Qu B and He T 2017 *Int.J.Hydrogen energy* **42** 4465-77
- [15] Zhu Y L, Sunarso J, Zhou W, Jiang S S and Shao Z P 2014 *J. Mater. Chem. A* **2** 15454-62
- [16] Lee K T and Manthiram A 2005 *Solid State Ionics* **176** 1521